Biochimica et Biophysica Acta 1818 (2012) 609–616

Contents lists available at SciVerse ScienceDirect

Biochimica et Biophysica Acta

journal homepage: www.elsevier.com/locate/bbamem

Structure, dynamics, and hydration of POPC/POPS bilayers suspended in NaCl, KCl, and CsCl solutions

Piotr Jurkiewicz [a], Lukasz Cwiklik [a,b], Alžběta Vojtíšková [a], Pavel Jungwirth [b,*], Martin Hof [a,**]

[a] J. Heyrovský Institute of Physical Chemistry, Academy of Sciences of the Czech Republic, v. v. i., Dolejškova 3, 18223 Prague 8, Czech Republic
[b] Institute of Organic Chemistry and Biochemistry, Academy of Sciences of the Czech Republic, and Center for Biomolecules and Complex Molecular Systems, Flemingovo nám. 2, 16610 Prague 6, Czech Republic

ARTICLE INFO

Article history:
Received 30 August 2011
Received in revised form 9 November 2011
Accepted 28 November 2011
Available online 6 December 2011

Keywords:
Solvent relaxation
Time-dependent fluorescence shift
Molecular dynamics simulation
Specific ionic effect
Anionic/zwitterionic phospholipid bilayer
Model lipid membrane

ABSTRACT

Effects of alkali metal chlorides on the properties of mixed negatively charged lipid bilayers are experimentally measured and numerically simulated. Addition of 20 mol% of negatively charged phosphatidylserine to zwitterionic phosphatidylcholine strengthens adsorption of monovalent cations revealing their specificity, in the following order: $Cs^+ < K^+ < Na^+$. Time-resolved fluorescence solvent relaxation shows significant decrease both in mobility and hydration of the lipid carbonyls probed by Laurdan upon addition of the cations. The experimental findings are supported by molecular dynamics simulations, which show deep penetration of the cations down to the glycerol level of the lipid bilayer where they pair with oxygen atoms of carbonyl groups (with pairing with *sn*-2 carbonyl being about twice stronger than pairing with the *sn*-1 one). Moreover, the cations bridge neighboring lipids forming clusters of up to 4 lipid molecules, which decreases the area per lipid, thickens the membrane, causes rising of lipid headgroups, and hinders lipid dynamics. All these effects follow the same Hofmeister ordering as the cationic adsorption to the bilayer.

© 2011 Elsevier B.V. All rights reserved.

1. Introduction

The lipid bilayer, which represents the core of all biological membranes, is a self-assembled structure composed of various amphiphilic lipids and water. Stability of this dynamical supramolecular aggregate is maintained by the interplay of several types of weak interactions, including interfacial tension resulting from the hydrophobic effect, steric repulsion between aliphatic chains, van der Waals interactions, and hydrogen bonding and complex electrostatics in the headgroup region [1–3]. Physical properties of the lipid bilayer are thus easily affected by various factors, such as the degree of hydration, lipid composition, membrane-associated proteins and sugars, as well as by the ions dissolved in the cytosol and extracellular fluid.

The influence of physiologically relevant ions (Na^+, K^+, Cl^-, Ca^{++}, or Mg^{++}) on model lipid membranes was studied extensively [4,5]. Other ions, such as Li^+, Cs^+, NH_4^+, Ba^{++}, La^{+++}, F^-, Br^-, I^-, NO_3^-, and SCN^- were also investigated [6,7] to elucidate the factors influencing the specific ionic effects observed. This specificity is known to be more pronounced for anions than for cations and, consequently, experimental data on cationic effects are sparser [7–10]. In contrast, computer simulations are less frequently focused on anions, since a proper description of the effects of larger anions often requires a resource-consuming polarizable force field [11], whereas appreciable specific interactions of cations with model membranes have been simulated using non-polarizable potentials [12–15]. The strongest are the effects of multivalent and monovalent cations with large charge density, such as Ca^{++} or Li^+, which are observed in both experiment and simulations [7,16]. Those cations bind to neutral (zwitterionic) lipid bilayers [6,17], rigidifying them [18] and stabilizing their gel phase [18–20]. Association of larger monovalent cations, like Na^+, K^+, Rb^+, and Cs^+, with a neutral lipid bilayer is much weaker and thus it is difficult to measure any differences between their effects [7,10]. Previous fluorescence measurements using solvent relaxation technique (SR) have shown weak dehydration and hindered mobility at the glycerol level of DOPC membrane upon addition of 150 mM NaCl [14], but similar effects have been observed also for other salts (KCl, CsCl, and NH_4Cl; unpublished data). Molecular dynamics simulations showed that Na^+, in contrast to K^+ or Cs^+, exhibits affinity to the headgroups of DOPC membrane and that it also attracts Cl^- from solution such that an electric double layer is created [14,21]. The binding site of Na^+ was found to be force field dependent ranging from phosphodiester to carbonyl groups of phospholipids [4,14,21,22]. The cationic effects are amplified in negatively charged membranes. For example, electrophoretic mobilities of phosphatidylserine (PS) noticeably differs in solutions of different alkali chlorides, yielding intrinsic association constants of 0.6, 0.15, and 0.05 M^{-1} for Na^+, K^+, and Cs^+, respectively [23]. In contrast to Li^+, which in this respect resembles divalent cations, no shifts in phase transition

* Corresponding author. Tel.: +420 220 410 314; fax: +420 220 410 320.
** Corresponding author. Tel.: +420 266 053 264; fax: +420 286 582 677.
E-mail addresses: piotr.jurkiewicz@jh-inst.cas.cz (P. Jurkiewicz), lukasz.cwiklik@jh-inst.cas.cz (L. Cwiklik), bibijone@gmail.com (A. Vojtíšková), pavel.jungwirth@uochb.cas.cz (P. Jungwirth), martin.hof@jh-inst.cas.cz (M. Hof).

0005-2736/$ – see front matter © 2011 Elsevier B.V. All rights reserved.
doi:10.1016/j.bbamem.2011.11.033

temperatures were measured for Na^+ and K^+ and no structural changes have been observed using X-ray diffraction [24]. This agrees with unhindered mobility of phosphodiester group of PS upon addition of Na^+ observed using ^{31}P NMR, interpreted as result of weak interactions of Na^+ with various PS bilayers [25]. MD simulations of POPS in NaCl provide an alternative scenario showing strong binding of Na^+ to lipid carbonyls, which may be undetectable using ^{31}P NMR [26]. Yet another MD study shows a broad distribution of Na^+ at the phosphate region of DMPS [27].

While still negatively charged, physiologically more important are mixed anionic/zwitterionic lipid bilayers, such as the POPC/POPS mixture. 20 mol% of POPS in POPC is a commonly used simple model of the inner lipid leaflet of a plasma membrane. Nevertheless, few studies addressed interactions of anionic/zwitterionic lipid bilayers with monovalent cations [15,28–31]. It was shown in MD simulations that sodium binds to headgroups of POPC/POPS bilayer, but no consensus regarding exact Na^+ location has been established [15,28,29]. Complexes of up to 4 lipid molecules were found with either carboxylate-Na-carboxylate or carboxylate-Na-phosphate salt bridging [28,29]. Electrophoretic mobility measurements of vesicles formed from phosphatidylcholine, phosphoinositol, and cholesterol resulted in an ion adsorption constant series of 2.18, 2.22, 3.03 mol^{-1} for Na^+, K^+, and Cs^+, respectively [30] (i.e., opposite order to that published in [23]).

The above brief review of the literature dealing with monovalent cations in zwitterionic, anionic, and mixed anionic/zwitterionic membranes thus points to a number of open questions concerning ion affinities, binding sites within the bilayer, and membrane structural changes. In order to address these issues, we investigate in the present study interactions of Na^+, K^+, and Cs^+ with mixed POPC/POPS lipid bilayers using fluorescence solvent relaxation technique (SR) and empirical force-field MD simulations. SR provides a unique tool for measuring hydration and local dynamics in the fully hydrated free-standing unilamellar lipid membranes, while MD reveals molecular structure of the bilayer and dynamical interactions between lipids and ions.

2. Methods

2.1. Experimental methods

2.1.1. Materials

1,2-palmitoyl-oleoyl-*sn*-glycero-3-phosphocholine (POPC) and 1,2-palmitoyl-oleoyl-*sn*-glycero-3-phosphoserine (POPS) were obtained from Avanti Polar Lipids (Alabaster, AL, USA). A fluorescence probe, 6-dodecanoyl-2-dimethylaminonaphthalene (Laurdan) was purchased from Molecular Probes (Eugene, OR, USA). NaCl and CsCl with purity >99%, NaOH, and ethylenediaminetetraacetic acid (EDTA) were obtained from Sigma Aldrich (St. Louis, USA), and KCl with purity ≥98% from Fluka (Buchs, Switzerland). Organic solvents of spectroscopic grade were supplied by Merck (Darmstadt, Germany). Salts and EDTA were dissolved in Mili Q (Milipore, USA) water. pH of EDTA solution was adjusted to 7.0 using NaOH. All chemicals were used without further purification.

2.1.2. Vesicle preparation

Chloroform solutions of appropriate lipids were mixed with Laurdan dissolved in methanol (1:100 dye:lipid molar ratio). The organic solvents were evaporated under a stream of nitrogen while being continuously heated. The lipid film was suspended in water with 0.1 mM EDTA or 1 M salt solution and vortexed for 3 min. EDTA was used to chelate calcium ions dissolved from the glassware. Large unilamellar vesicles (LUVs) were prepared by extrusion through a polycarbonate membrane (Avestin, Ottawa, Canada) with 100 nm pores. The prepared samples were transferred to a 1 cm quartz cuvette. The final concentration of phospholipids in the cuvette was 1 mM.

2.1.3. Fluorescence instrumentation

All steady-state fluorescence measurements were performed on a Fluorolog-3 spectrofluorimeter (model FL3-11; Jobin Yvon Inc., Edison, NJ, USA). Fluorescence decays were recorded on an IBH 5000 U SPC equipped with an IBH laser diode NanoLED 11 (370 nm peak wavelength, 80 ps pulse width, 1 MHz repetition rate) and a cooled Hamamatsu R3809U-50 microchannel plate photomultiplier. The temperature was maintained at 283 K or 293 K ± 0.5 K using a water-circulating bath. The full width at half maximum (FWHM) of the instrument response function was less than 100 ps.

2.1.4. Fluorescence solvent relaxation

A detailed description of the fluorescence solvent relaxation method, also called time-dependent fluorescence shift (TDFS), and its application to characterization of phospholipid bilayers, can be found in the recent review [32]. The primary data consist of a steady-state emission spectrum and a set of emission decays recorded at a series of emission wavelengths (400–540 nm with 10 nm step). The time-resolved emission spectra (TRES) were gained by the spectral reconstruction method [33]. Positions of TRES maxima, $\nu(t)$ and their $FWHM(t)$ were analyzed. The position of TRES maximum at $t=0$ was estimated according to the method of Fee and Maroncelli [34] as $\nu(0)=23{,}800\ cm^{-1}$ and was not affected by the presence of ions. Two main parameters describing polarity and mobility of the probed system are derived from the analysis of TRES. The total emission shift $\Delta\nu=\nu(0)-\nu(t=\infty)$ directly reflects the polarity of the dye microenvironment, while integrated mean relaxation time, defined as $\tau=\int_0^\infty \frac{\nu(t)-\nu(\infty)}{\Delta\nu}dt$, describes the mobility of polar moieties in the vicinity of the fluorophore. The percentage of the relaxation process that was faster than the time resolution of the instrumentation (~20 ps), calculated as $(\nu_e(0)-\nu_m(0))/(\nu_e(0)-\nu(\infty))$, where e and m index $\nu(0)$ values obtained from the time-zero spectrum estimation and from TRES reconstruction, respectively, did not exceed 15% for any of the samples measured at 283 K, and 25% for those measured at 293 K.

2.2. Computational methods

Molecular dynamics simulations were performed for bilayers of 128 lipid molecules (64 molecules in each leaflet) hydrated with over 4200 molecules of water. A POPC bilayer was equilibrated for 50 ns. Then, 26 POPC molecules (13 lipids selected randomly in each leaflet) were exchanged for POPS molecules resulting in 20 mol% concentration of POPS. In order to neutralize the charge of anionic lipids, 26 monovalent cations (Na^+, K^+, or Cs^+) were added to the aqueous phase. Additional cations and chloride anions were added to the aqueous phase in order to achieve a formal 1 M salt concentration (not counting the neutralizing cations). The overall resulting concentration of cations in water phase (calculated from the ratio of ions to water molecules) amounted to 1.4 M, whereas concentration of chloride anions was 1 M. The three resulting systems thus consisted of 106 monovalent cations and 80 Cl^- anions, and corresponded to the mixed POPC + 20 mol% POPS membranes hydrated with 1 M solution of NaCl, KCl, or CsCl. For each system a molecular dynamics trajectory of 200 ns length was calculated. For time-independent analyses only the final 50 ns of the trajectories were used.

Lipid molecules were modeled employing the Berger's nonpolarizable united-atom empirical force-field [35]. The SPC model of water, for which Berger's parameterization was developed, was used [36]. Parameters for ions were taken from the GROMACS force-field [37], however, for K^+ we employed parameters introduced by Vacha et al. [38], which correct the unrealistically small depth of the Lennard–Jones potential of potassium in the original GROMACS force-field. Simulations were performed in the isothermal–isobaric ensemble (NpT) with the temperature coupling using the Nose–Hoover

thermostat [39] at 310 K and with pressure of 1 bar controlled in a semi-isotropic setup by the Parrinello–Rahman barostat [40]. Non-bonded interactions were cut off at 1 nm, with the long-range electrostatic interactions accounted for employing the Particle Mesh Ewald method with grid spacing of 0.12 nm and fourth-order interpolation [41]. Water molecules were constrained employing the SETTLE algorithm and the LINCS algorithm was used for constraining bonds in lipid molecules [42,43]. Equations of motions were integrated with a 2 fs time step. Calculations were performed employing the GROMACS 4.0.7 software package [37].

3. Results and discussion

Lipid bilayers consisting of 20 mol% of POPS and 80 mol% of POPC (POPC/POPS) suspended in NaCl, KCl, or CsCl solution were studied using SR fluorescence technique and MD simulations. Comparison with pure POPC bilayer is based on separate measurements and literature data (in the case of MD [13]). In fluorescence measurements 1 mol% of lipid was replaced with a fluorescent polarity probe — Laurdan. The structures of the employed compounds and the location of the fluorescent probe are shown in Fig. 1. Experimental and computational results are presented and discussed together, with the material divided into sections based on different aspects of salt-bilayer interactions rather than on the method used to obtain the result. First, the changes in bilayer mobility at the glycerol level, as probed by Laurdan, and structural changes revealed by MD are analyzed. Further, we focus on cations themselves, the depth of their penetration into the bilayer, their binding sites, and clustering effects. Finally, changes in bilayer hydration are discussed.

3.1. Hindered dynamics at the glycerol level

SR gives a unique possibility to measure local polarity and mobility at different depths of fully hydrated liquid crystalline lipid bilayers, which is a valuable model of biological membranes. Fluorescence quenching methods and computer simulations have shown that Laurdan, used in the present study, is stably located at the glycerol level of phospholipid bilayer [44,45]. At this depth all water molecules are bound to lipids and thus the observed nanosecond relaxation should be attributed to the motion of the whole hydrated phospholipid moieties rather than water molecules themselves, which in the bulk relax about 10^4 times faster [46]. Laurdan was shown to be particularly sensitive to the dynamics of the hydrated *sn*-1 carbonyls of phosphatidylcholine bilayer [47].

SR measurements were performed at 283 K and 293 K. At both temperatures each of the investigated bilayers was in a liquid–crystalline state. Low temperature was used to increase the extent of relaxation process captured with the time resolution of the instrumentation. Below we primarily discuss the measurements performed at 283 K, where the effects are more pronounced. At 293 K no qualitative differences between the samples have been observed, although the effects were less apparent due to larger uncertainty of the measurements.

Positions of the maxima of TRES, $\nu(t)$, representing the relaxation process measured at 283 K are shown in Fig. 2. The relaxation curves obtained for the POPC bilayer and the POPC/POPS bilayer in pure water are very similar. For POPC, the mobility at the glycerol level was only slightly slower for 1 M alkali chloride solutions, regardless of the cation present, when compared to pure water. As opposed to neutral POPC, in the negatively charged POPC/POPS bilayer strong specific cationic effects were observed. The relaxation slows down considerably reporting a restricted mobility at the glycerol level of POPC/POPS. The mobility is in the order: water > CsCl > KCl > NaCl. The values of integrated relaxation times τ are listed in Table 1. The presence of sodium slows down mobility at 283 K by 42% when compared to water, while cesium only by 23%; at 293 K the effects are smaller: analogous values are 21% and 14%, respectively. These are unexpectedly large changes when compared to the previously published data of the effects of small cations in neutral membranes [11,14]. Introduction of physiologically relevant amount of POPS thus not only limits mobility of the POPC/POPS bilayer at its glycerol level in each of the studied salt solutions, but also reveals cation specificity.

Since in pure water no significant differences in relaxation dynamics between the POPC and the POPC/POPS systems were observed, the electrostatic repulsion predicted between PS headgroups is apparently compensated. Likely factors that can prevent membrane expansion upon addition of POPS are stronger hydrogen bonding in POPC/POPS bilayer, smaller volume of PS headgroup, and the presence of PS counterions (in our experiment it resulted in a 0.2 mM concentration of Na^+). In fact, measurements performed at 293 K show that addition of POPS might even restrict the mobility of POPC bilayer (see Table 1). For all

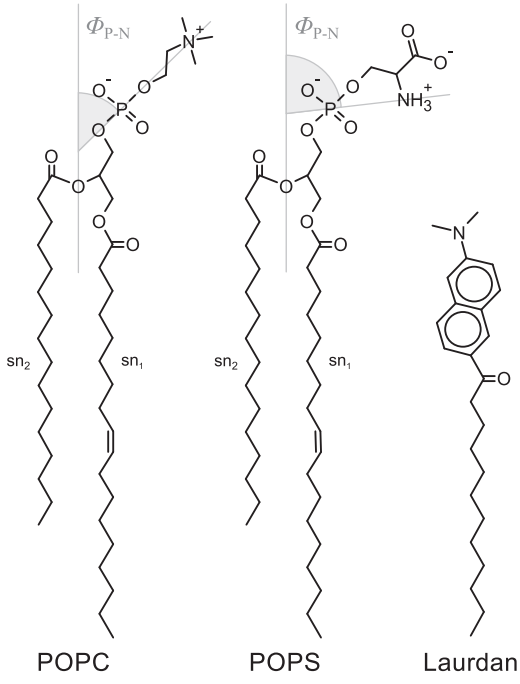

Fig. 1. Chemical structures of neutral POPC, anionic POPS, and the fluorescent probe Laurdan. $\Phi_{P\text{-}N}$ angles between P–N dipoles and the membrane normal, and sn_1 and sn_2 chains are marked both for POPC and POPS molecules. Laurdan fluorophore is located in accord with the parallax quenching results [44] and computer simulations [45].

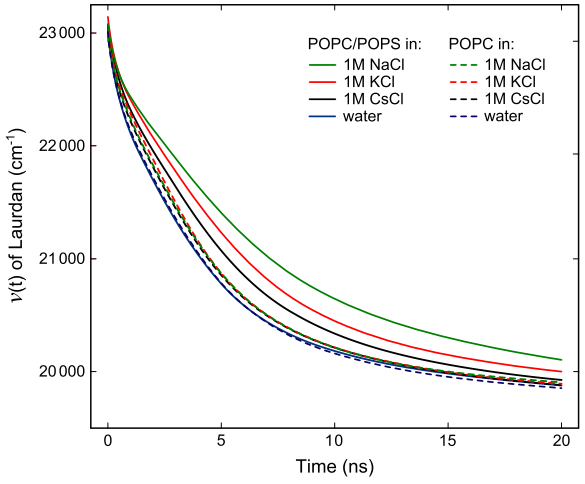

Fig. 2. Position of the maxima of time resolved emission spectra of Laurdan embedded in POPC or POPC/POPS (4:1) large unilamellar vesicles suspended in water or 1 M salt solutions. Note that the curves obtained for POPC in different salt solutions are almost indistinguishable.

Table 1
Numerical results obtained from both solvent relaxation (SR) measurements using 1 mol% of Laurdan as a fluorescent probe and molecular dynamics (MD) simulations.

Lipid	Solution (1 M)	$\Delta\nu$ (cm^{-1})[a]		τ (ns)[b]		<APL> (nm^2)[c,f]	<z_{P-P}> (nm)[d,f]	<Φ_{P-N}> (deg)[e,f]	
		283 K	293 K	283 K	293 K			POPC	POPS
POPC/POPS (4:1)	NaCl	3700	4050	4.50	2.61	0.546	2.16	55.7	81.7
	KCl	3800	4075	4.16	2.56	0.561	2.17	55.3	78.7
	CsCl	3850	4075	3.90	2.46	0.607	1.97	67.3	83.4
	Water	3925	4100	3.17	2.15	–[g]	–[g]	–[g]	–[g]
POPC	NaCl	3900	4050	3.41	2.02	0.608[h]	2.0[h,i]	69.6[h,j]	–
	KCl	3900	4050	3.40	2.07	0.639[h]	1.9[h,i]	74.2[h,j]	–
	CsCl	3900	4050	3.37	1.99	–	–	–	–
	water	3950	4075	3.22	1.78	0.654 0.652[h]	1.92	70.5 77.9[h,j]	–

[a] (SR) total emission shift, $\Delta\nu = \nu(0) - \nu(\infty)$; where $\nu(0) = 23{,}800\ cm^{-1}$ estimated according to [34], and $\nu(\infty)$ obtained from TRES reconstruction.

[b] (SR) integrated relaxation time: $\tau = \int_0^\infty \frac{\nu(t)-\nu(\infty)}{\Delta\nu} dt$.

[c] (MD) mean bilayer area per lipid molecule.

[d] (MD) bilayer thickness calculated as a mean distance between PO_4 groups of opposite leaflets.

[e] (MD) mean angle between headgroup P–N dipole and the membrane normal, see Fig. 1.

[f] Calculated based on the final 50 ns of trajectories.

[g] Even in water the system contains counteractions neutralizing POPS, and such a low ion concentration regime cannot be effectively studied in simulations.

[h] Taken from Ref. [13], where 0.2 M salt concentrations were used, with CHARMM force-field employed for ions and Berger's force-field for lipids.

[i] Estimated from density profiles shown in Fig. 3 in Ref. [13] with CHARMM force-field employed for ions.

[j] Values obtained directly from angle histograms as opposed to the normalized ones calculated in the present work, see text for details.

the measured samples the width of TRES, i.e., FWHM was carefully analyzed. No signs of heterogeneity in Laurdan relaxation were present, since all FWHM profiles exhibited single maxima at the times corresponding to the integrated relaxation time (data not shown).

3.2. Bilayer compression and rising of POPC headgroups

Molecular dynamics simulations have shown that adding 1 M of the studied salt solutions significantly decrease the area per lipid (APL) of the POPC/POPS bilayer. Fig. 3 illustrates calculated APL values; for comparison we also show the average values for pure-POPC membrane in ion-free water, 0.2 M NaCl, and 0.2 M KCl based on simulations by Gurtovenko and Vattulainen employing CHARMM force-field for ions [13]. The stabilization time of APL along the trajectory depends on the type of salt. In the CsCl solution the area per lipid stabilizes after about 20 ns, in the case of NaCl the stabilization takes about 100 ns, and in the case of KCl a full stabilization was not observed even after 200 ns.

The observed influence of salts on APL increases in the order CsCl<KCl<NaCl. Since the SR relaxation time τ of Laurdan is typically inversely proportional to the area per lipid, the simulated APL agree well with the measured relaxation time, i.e., the smaller the APL the more hindered the dynamics probed by Laurdan.

The POPC/POPS membrane compression has been already observed in MD simulations upon adhesion of Na^+ or Ca^{++} ions [15,28], but no specific cation effects have been reported. A similar but much weaker cation specificity of membrane compression was shown in our previous study of a neutral DOPC bilayer, where APL was 0.72, 0.70, 0.69, and 0.69 nm^2 for water, 1 M CsCl, KCl, and NaCl, respectively [14]. Those results agree well with the SR times obtained here for pure POPC. Note that in the case of DOPC the change in compression between CsCl and NaCl was only about 1.4% as opposed to 10% in the case of POPC/POPS discussed here. Absolute comparison is, however, not possible since the DOPC backbone has a larger volume than that of POPC, which may, to some extent, hinder headgroup interactions. Neither are the results obtained by Gurtovenko et al. presented in Table 1 an ideal reference due to the different force field and salt concentration used there. Nevertheless, we can safely conclude that in the presence of POPS the effect of cations is markedly enhanced. The decrease of the APL in the POPC/POPS system caused by the weakly-interacting CsCl is comparable to that induced by the strongly-interacting NaCl on pure POPC. Also, in the POPC system KCl causes only a slight decrease of the area per lipid, and one can expect that the effect induced by CsCl (not included in the pure-POPC study) would be even smaller.

Density profiles calculated for the three considered salt solutions are depicted in Fig. 4. It is apparent that the bilayer in NaCl and KCl solutions is thicker than in CsCl. The mean thickness, z_{P-P}, calculated as the distance between phosphates of the opposed leaflets is presented in Table 1. The changes of POPC/POPS bilayer thickness observed here are larger than those of pure POPC [13] or DOPC [14].

Note that for pure POPC membranes the empirical force-fields have tendency to overestimate the thickening of the bilayer in salt solutions, as experimentally almost no effect on the POPC bilayer thickness can be observed for salt concentration below 1 M [18] whereas in simulations membrane thickening occurs already in 0.2 M salt solutions. On top of the increased distance between opposing phosphates, the overall POPC/POPS membrane thickness is further increased by the rising of

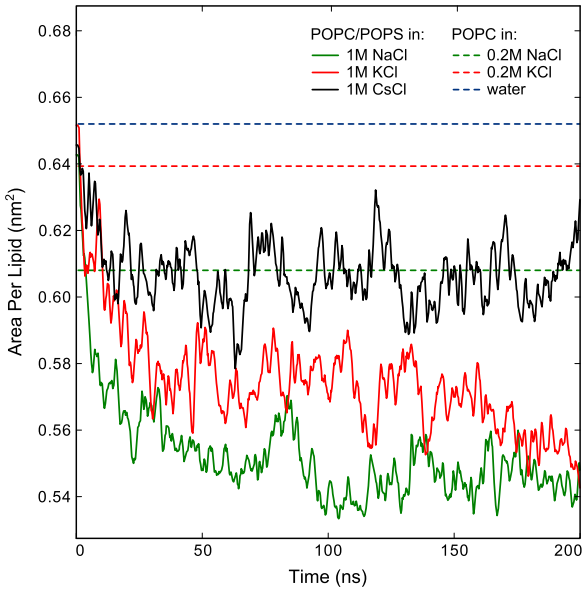

Fig. 3. Area per lipid (APL) as a function of simulation time. Dashed lines depict average values of area per lipid for pure-POPC bilayer taken from Ref. [13] and corresponding to the values calculated employing the CHARMM force-field for ions. The numerical results are gathered in Table 1.

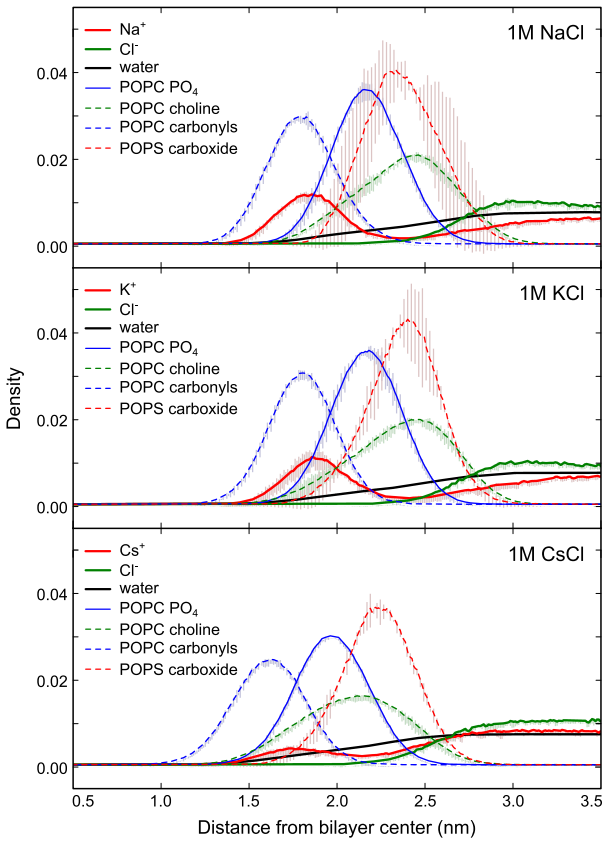

Fig. 4. Relative partial density profiles calculated over last 50 ns of trajectories. The density profiles for both leaflets are averaged. The values of variance are used as error bars. For clarity of presentation, each profile is normalized to give the same integral. The profiles are cut at the distance of 3.5 nm from the bilayer center. Absolute density profiles of ions are depicted in Fig. 2S in the Supporting information.

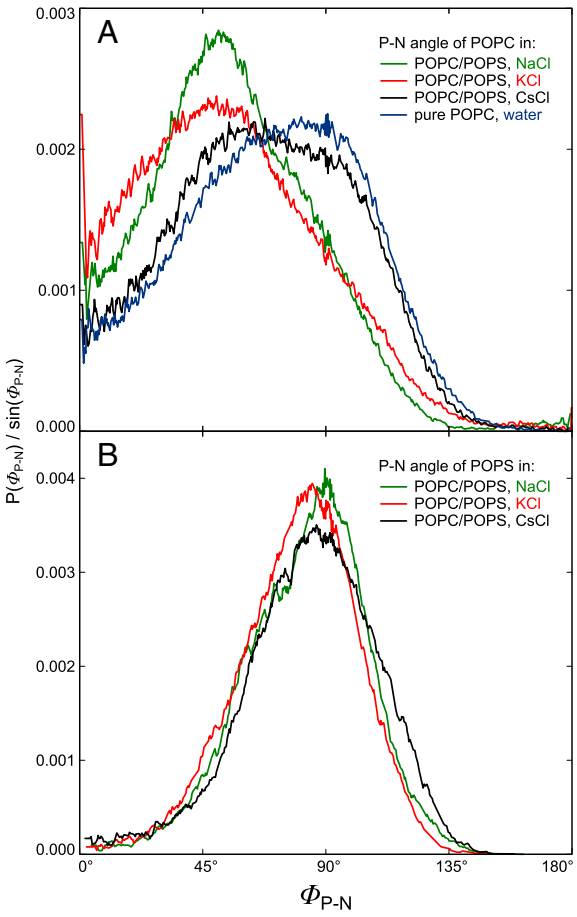

Fig. 5. Normalized distributions of Φ_{P-N} headgroup angles (see Fig.1) of POPC (A) and POPS (B) calculated based on final 50 ns of MD trajectories; 0° represents P–N dipoles pointing outward of the membrane and 180° toward membrane interior.

the POPC headgroups, i.e., the POPC P–N dipole, which is typically laying flat on the membrane surface, reorients in the presence of KCl and NaCl. This effect can be already observed in Fig. 4, in which the density peak of choline shifts outward from the center of the bilayer; becoming also narrower. The distributions of the angle between the P–N dipole and the membrane normal, Φ_{P-N}, depicted in Fig. 5, illustrate this change in more details. The mean values of Φ_{P-N} are given in Table 1. The P–N dipole of POPC in the POPC/POPS membrane in CsCl solution has a broad distribution of Φ_{P-N} angles, similar to those of pure POPC in water (Fig. 5A), with mean values of 67° and 71°, respectively. Exchange of CsCl to either KCl or NaCl narrows the Φ_{P-N} distribution and shifts it toward lower angles; $<\Phi_{P-N}> \approx 55°$. Also, note the differences between $<\Phi_{P-N}>$ values obtained in Ref. [13] and in the present work. These are due to normalization applied by us, i.e. division of Φ_{P-N} histogram by $\sin(\Phi_{P-N})$ in order to obtain a properly normalized Φ_{P-N} distribution. The normalization broadens and shifts the distribution toward lower angles, e.g., for pure POPC in water the $<\Phi_{P-N}>$ values before and after normalization are 77.8° and 70.5°, respectively. The former one agrees with the unnormalized value of 77.9° published in [13]. In comparison with POPC, the Φ_{P-N} distributions for POPS are almost identical for the three salt solutions with a narrow peak around 90° (see Fig. 5B), indicating that the P–N axis is oriented roughly parallel to the surface.

3.3. Location of ions

Molecular dynamics simulations reveal deep penetration of cations into the POPC/POPS bilayer; see density profiles in Fig. 4. The density of cations is non-negligible as deep as about 1.4 nm from the center of the lipid bilayer, which corresponds to the position of POPC carbonyls at the glycerol level. As a matter of fact, the peaks of cation densities are located close to the position of peaks of the carbonyls. The corresponding peak intensities and thus the preference toward carbonyl groups increase in the order $Cs^+ < K^+ < Na^+$. In contrast, chloride anions are not adsorbed at the membrane but rather stay in the aqueous phase. In the case of NaCl and KCl solutions the distribution of chloride has a weak peak at about 2.9 nm from the center of the lipid bilayer while this peak is absent for CsCl. The region between cation-enriched parts of the membrane and anion-enriched aqueous phase is predominantly occupied by both choline and carboxylate groups. Separation between anions and cations is enhanced by the presence of carboxylate groups of POPS molecules as these negatively charged groups repel anions. This can be demonstrated by plotting the distribution of charges due to individual components of the system along the membrane normal (see Fig. S1 in the Supplementary information). Indeed, chloride anions are repelled from the membrane by negatively charged headgroups of POPS lipids whereas metal cations are predominantly occupying the region of negatively charged carbonyl groups of POPC. A qualitatively similar separation of cations and anions was observed in neutral zwitterionic membranes, including the POPC bilayer, which demonstrates that the presence of anionic lipid is not necessary for charge separation in salt solutions [11–14,26], although, the effect is enhanced by the presence of POPS. In the simulated system, the electroneutrality in the water phase (the equality of cation and anion concentrations) is established ~1.2–1.6 nm from the membrane–water interface (see Fig. 2S in the Supplementary information). In that region, concentrations of ions amount for 1.09, 1.18, and 1.36 M in, accordingly, NaCl, KCl, and CsCl solution. The increase of the ionic concentration in this region with regard to the formal 1 M concentration of the salt in the system

results from the repulsion of anions from the negative bilayer. The results of present simulations can thus be directly compared with the experimental data obtained at salt concentrations in the approximate range of 1–1.4 M.

3.4. Extent of cationic adsorption and ion-lipid contacts

Radial distribution functions between the studied cations and oxygen atoms of carbonyls, phosphates, and carboxyls from MD simulations are depicted in Fig. 6. The binding of cations with the carbonyl groups is prevailing; and the carbonyl groups located at the *sn*-2 chain of POPC are binding the cations more strongly than the carbonyls at the *sn*-1 chain (compare Fig. 6A and B). The preferential binding with carbonyl groups increases in the series $Cs^+<K^+<Na^+$, while the preferential distance between carbonyl oxygen atoms and cations changes correspondingly to the ionic radius ($Na^+<K^+<Cs^+$). Radial distribution functions show binding of cations with both phosphate groups of POPC/POPS and carboxylate groups of POPS (see low-intensity peaks located in the 0.2–0.4 nm region in Fig. 6C, D); however, as evident from the values of cumulative sum, this binding is weak in comparison with the binding of cations by carbonyl groups. In the case of both carboxyl and phosphate groups, small contact peaks are accompanied by more pronounced peaks at the larger distances; however, the latter originate from these cations which are already bound by carbonyl groups of a corresponding lipid molecule.

In order to quantify the affinity of ions toward the membrane we analyzed average coordination numbers between ions and a given type of lipid atoms. This quantity was calculated as a number of ions corresponding to a first peak of the radial distribution functions (compare insets in Fig. 6). It approximately accounts for the first solvation shell for each of considered types of atomic pairs. Note that the coordination numbers reflect the local neighborhood of the considered atom, in contrast to the density profiles discussed above, which represent spatially-averaged distributions of species in the system. The number of cations corresponding to first peaks around the *sn*-2 carbonyl group is approximately equal to 0.7, 0.5, and 0.2 for Na^+, K^+, and Cs^+, correspondingly. The average coordination numbers of carbonyl groups at the sn-1 chain are lower (0.15, 0.2, and 0.1 for Na^+, K^+, and Cs^+, accordingly), with the value for potassium slightly above that for sodium. The preference of ions toward *sn-2* carbonyl groups over *sn-1* groups can be rationalized by differences in localization of both *sn-2* and *sn-1* carbonyls, with the former being located closer to the headgroup region and hence being more hydrated and accessible for ions [48]. Average coordination numbers for both phosphate and carboxylic numbers are significantly, almost one order of magnitude, smaller than those of carbonyl groups. However, the trend in the ion binding ($Cs^+<K^+<Na^+$) is the same as in the case of carbonyl groups. We also analyzed the life-time characteristic for complexes formed between carbonyl groups of POPC and cations. The average life-time of the cation–oxygen pairs studied employing the time autocorrelation functions strongly varies depending on the type of cation, it is in a range of about 25 ns for cesium, in the range of 40 ns for potassium and even longer for sodium. In the case of both potassium and sodium one can speak about strong ion pairing with *sn*-2 carbonyl groups, as evident from relatively high peaks of the corresponding radial distribution functions depicted in Fig. 6B.

As mentioned in the Introduction, different cation binding sites were reported in the literature based on molecular dynamics simulations employing different force-fields. Several studies, including this one, predict the binding of Na^+ by carbonyl oxygen atoms PC lipids [4,13,22,26]. In other works, the concentration of sodium cations was found to be maximized in the vicinity of phosphate groups [14,27]. Yet other authors report that Na^+ penetrates between the region of phosphate groups and carbonyls [27]. Moreover, complexes of up to 4 lipid molecules were found with either carboxylate-Na-carboxylate or carboxylate-Na-phosphate salt bridging [28,29]. The

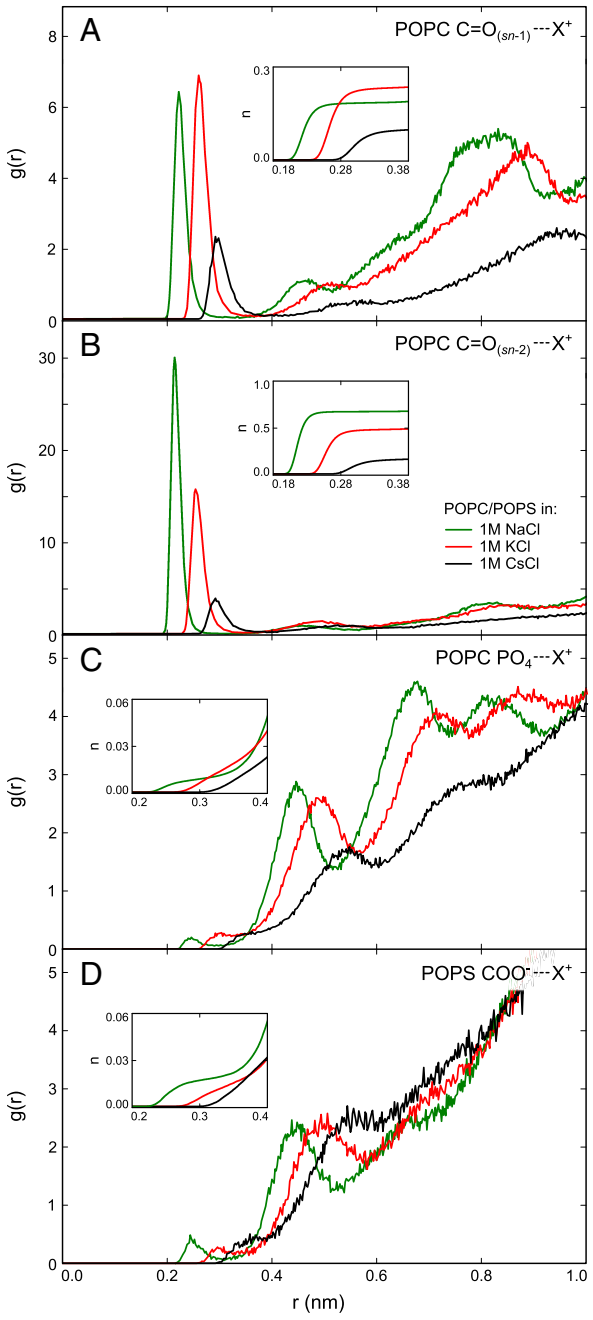

Fig. 6. Radial distribution functions for atomic pairs between the studied metal cations and oxygen atoms of (A) *sn*-1 and (B) *sn*-2 carbonyls, (C) phosphate group of POPC, and carboxylate group of POPS. The distributions were calculated over last 50 ns of trajectories. Normalization to the ideal gas density was not employed, since the membrane/water interface is an inhomogeneous system. The values of cumulative sums are depicted in insets.

stronger preference of cations for carbonyl than phosphate groups is supported by the present fluorescence measurements since the influence of cations on membrane properties and the dependence on the cation type was observed employing Laurdan fluorophore which probe *sn-1* carbonyl atoms of a phospholipid [6].

Carboxylate groups of POPS are significantly exposed to the water phase. One could naively expect that the binding of cations by anionic $-COO^-$ moieties would be more significant than between carbonyl groups and cations. Factors which contribute to this relatively low cation binding are the presence of neighboring positively charged choline groups and the tendency for formation of both intra- and

intermolecular hydrogen bonds between them and $-COO^-$ groups; such hydrogen bonds were also reported in previous studies of POPS membranes [26].

A bridging effect of lipid molecules by a sodium cation was already reported both from simulations [4,49,50] and experiments [51]. It was concluded that a sodium cation may effectively bind more than one carbonyl group thus allowing for bridging between nearest neighboring lipid molecules. Fig. 7 presents distributions of numbers of lipids forming clusters formed by carbonyl-cation-carbonyl interactions (both POPC and POPS lipids are considered). Among the cations which form clusters, most of them bind more than one lipid molecule. Both sodium and potassium cations predominantly form complexes with three lipids (in accord with a previous study of sodium salt in membranes [39], while four-lipid clusters were reported in other studies [4,49,50]), whereas two-lipid complexes are the most abundant in the membrane interacting with cesium cations. For each cation the distribution of the cluster sizes is broad, up to complexes involving five lipid molecules, with the sodium cation being the most effective in clustering, followed by potassium, and cesium.

3.5. POPC/POPS carbonyls dehydration upon cation adsorption

Both SR measurements and MD simulations show a certain degree of dehydration of POPC/POPS bilayer carbonyls in 1 M salt solutions. Hydrating water is the main constituent of the dipolar relaxation probed by Laurdan, thus the emission shift $\Delta\nu$ is usually attributed to hydration of carbonyls at the glycerol level. The $\Delta\nu$ values obtained for the measured POPC/POPS and pure POPC vesicles are shown in Table 1. Hydration of POPC/POPS carbonyls strongly decreases in the order: pure water > CsCl > KCl > NaCl. This is not observed for pure POPC, where the changes are within the experimental error, and only a slight dehydration is observed upon addition of salt (water ≥ CsCl = KCl = NaCl). The hydration effects at 293 K are considerably smaller than the ones measured at 283 K. It is important to mention that $\Delta\nu$ is usually less sensitive than the second SR parameter, τ. The observed level of dehydration, namely a 250 cm^{-1} difference between POPC/POPS in water and in 1 M NaCl at 283 K is remarkably large. When comparing the two lipid system studied, it is apparent that introduction of POPS into neutral POPC membrane dehydrates the membrane at the *sn*-1 carbonyl, whenever any of the studied salt is present. POPS also enhances the differences in the dehydration between the studied monovalent cations. In the absence of salt, introduction of POPS does not affect the hydration.

Corresponding changes of membrane hydration, measured at the level of carbonyl groups, were observed also in MD simulations. Fig. 8 depicts radial distribution functions calculated for pairs formed between water molecules and carbonyl groups. The influence of the type of cation on the hydration is reflected in the changing intensity of the first peak of the radial distribution function. Hydration increases in the series $Na^+ < K^+ < Cs^+$ which is in accord with the present results of SR experiments.

In the recent calorimetric study it has been shown that absorption of alkali metal cations to phospholipid vesicles is endothermic, and thus entropy-driven process [52]. The authors hypothesize that the entropy gain is due to partial dehydration of both lipids and ions, which leads to the liberation of water molecules. Dehydration observed in the present study is in favor of this hypothesis.

4. Summary and conclusions

We observed strong specific effects of alkali cations on mixed POPC/POPS bilayers where the extent of adsorption, and thus the strength of the influence on the membrane, depends on the type of cation. The influence of cations increases in the series $Cs^+ < K^+ < Na^+$. This tendency is reflected in all bilayer properties described in the present study, both structural and dynamical ones. In pure zwitterionic membranes the cationic effects are weak (particularly when compared to anionic effects), however, in the mixed POPC/POPS system they are enhanced by the presence of the negatively charged lipids.

The presence of cations thus has a significant effect on the mixed POPC/POPS bilayer. The most apparent are the structural changes. The POPC/POPS bilayer undergoes a significant compression, as well as thickening and rising of the POPC headgroups. This is a direct consequence of extensive adsorption of cations. Our results, both from experiments and simulations, show that monovalent cations have a strong affinity toward oxygen atoms in the carbonyl groups and a weaker affinity toward the phosphate groups. Interactions between alkali cations and anionic headgroups of POPS are present, too. However, they are weaker than those with carbonyl groups due to the presence of nearby choline groups and intramolecular COO^-–choline pairing. As a result, anionic headgroups of POPS serve primarily as an "electrostatic spacer" between the cation-enriched carbonyl region of the bilayer and the anion-enriched water phase region next to the bilayer. Consequently, more cations undergo adsorption in the mixed POPS/POPC system than in the pure POPC bilayers.

The presence of monovalent salts results also in dehydration of the carbonyl region of the mixed POPC/POPS bilayer and a hindered dynamics

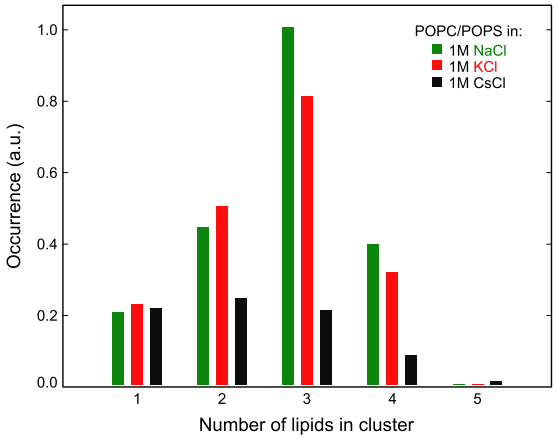

Fig. 7. Distributions of average numbers of oxygen-cation clusters formed by bridging of oxygen atoms of carbonyl groups of both POPC and POPS by cations. The 3.5 Å distance was taken as a criterion for the complex formation. Calculations were completed over last 50 ns of trajectories. Occurrence for 5-lipid complexes is equal to 2×10^{-5}, 8×10^{-4} and 3×10^{-3} for Na^+, K^+ and Cs^+, respectively.

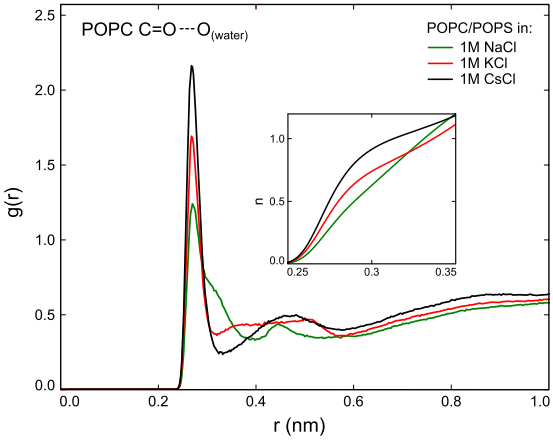

Fig. 8. Radial distribution functions (and integrals thereof — inset) calculated for atomic pairs between oxygen atoms of carbonyl groups in both *sn*-1 and *sn*-2 chains of POPC molecules and oxygen atoms of water molecules. Calculations were completed over last 50 ns of trajectories.

at the glycerol level, observed both in simulations and SR measurements. This results in a lower polarity and mobility in this region, affecting the dynamical properties of the mixed membrane. It is noteworthy that such a decrease in local polarity was not observed for the pure POPC system. Alkali cations (particularly sodium and, to a lesser extent, also potassium and cesium) also form bridges between lipid molecules, with a preference toward a 3-lipid complexes. Similar effects were previously observed for pure POPC bilayers. One may have expected that in the mixed POPC/POPS system the repulsive interactions between anionic POPS lipids would weaken the tendency for lipid clustering, however, no such weakening was observed. This may be a consequence of the effective screening of the repulsive interactions by the presence of cations in the aqueous phase.

Acknowledgement

Support from the Czech Science Foundation (EUROMEMBRANES project MEM/09/E006 and grant 203/08/0114), the Czech Ministry of Education grant (LC512 and LC06063), and the Academy of Sciences (Praemium Academie) is gratefully acknowledged.

Appendix A. Supplementary data

Supplementary data to this article can be found online at doi:10.1016/j.bbamem.2011.11.033.

References

[1] J.N. Israelachvili, S. Marcelja, R.G. Horn, Physical principles of membrane organization, Q. Rev. Biophys. 13 (1980) 121–200.
[2] M. Bloom, E. Evans, O.G. Mouritsen, Physical-properties of the fluid lipid-bilayer component of cell-membranes — a perspective, Q. Rev. Biophys. 24 (1991) 293–397.
[3] M. Langner, K. Kubica, The electrostatics of lipid surfaces, Chem. Phys. Lipids 101 (1999) 3–35.
[4] R.A. Böckmann, A. Hac, T. Heimburg, H. Grübmüller, Effect of sodium chloride on a lipid bilayer, Biophys. J. 85 (2003) 1647–1655.
[5] A. Filippov, G. Orädd, G. Lindblom, Effect of NaCl and $CaCl_2$ on the lateral diffusion of zwitterionic and anionic lipids in bilayers, Chem. Phys. Lipids 159 (2009) 81–87.
[6] A. McLaughlin, C. Grathwohl, S. McLaughlin, Adsorption of divalent-cations to phosphatidylcholine bilayer membranes, Biochim. Biophys. Acta 513 (1978) 338–357.
[7] J.J. Garcia-Celma, L. Hatahet, W. Kunz, K. Fendler, Specific anion and cation binding to lipid membranes investigated on a solid supported membrane, Langmuir 23 (2007) 10074–10080.
[8] W. Kunz, P. Lo Nostro, B.W. Ninham, The present state of affairs with Hofmeister effects, Curr. Opin. Colloid Interface Sci. 9 (2004) 1–18.
[9] S.A. Tatulian, Binding of alkaline-earth metal-cations and some anions to phosphatidylcholine liposomes, Eur. J. Biochem. 170 (1987) 413–420.
[10] R.J. Clarke, C. Lüpfert, Influence of anions and cations on the dipole potential of phosphatidylcholine vesicles: a basis for the Hofmeister effect, Biophys. J. 76 (1999) 2614–2624.
[11] R. Vacha, P. Jurkiewicz, M. Petrov, M.L. Berkowitz, R.A. Böckmann, J. Barucha-Kraszewska, M. Hof, P. Jungwirth, Mechanism of interaction of monovalent ions with phosphatidylcholine lipid membranes, J. Phys. Chem. B 114 (2010) 9504–9509.
[12] M.L. Berkowitz, D.L. Bostick, S. Pandit, Aqueous solutions next to phospholipid membrane surfaces: insights from simulations, Chem. Rev. 106 (2006) 1527–1539.
[13] A.A. Gurtovenko, I. Vattulainen, Effect of NaCl and KCl on phosphatidylcholine and phosphatidylethanolamine lipid membranes: insight from atomic-scale simulations for understanding salt-induced effects in the plasma membrane, J. Phys. Chem. B 112 (2008) 1953–1962.
[14] R. Vacha, S.W.I. Siu, M. Petrov, R.A. Böckmann, J. Barucha-Kraszewska, P. Jurkiewicz, M. Hof, M.L. Berkowitz, P. Jungwirth, Effects of alkali cations and halide anions on the dopc lipid membrane, J. Phys. Chem. A 113 (2009) 7235–7243.
[15] R.D. Porasso, J.J.L. Cascales, Study of the effect of Na^+ and Ca^{2+} ion concentration on the structure of an asymmetric DPPC/DPPC plus DPPS lipid bilayer by molecular dynamics simulation, Colloids Surf., B 73 (2009) 42–50.
[16] P.T. Vernier, M.J. Ziegler, R. Dimova, Calcium binding and head group dipole angle in phosphatidylserine-phosphatidylcholine bilayers, Langmuir 25 (2009) 1020–1027.
[17] H. Akutsu, J. Seelig, Interaction of metal-ions with phosphatidylcholine bilayer-membranes, Biochemistry 20 (1981) 7366–7373.
[18] G. Pabst, A. Hodzic, J. Štrancar, S. Danner, M. Rappolt, P. Laggner, Rigidification of neutral lipid bilayers in the presence of salts, Biophys. J. 93 (2007) 2688–2696.
[19] D. Chapman, W.E. Peel, B. Kingston, T.H. Lilley, Lipid phase-transitions in model biomembranes — effect of ions on phosphatidylcholine bilayers, Biochim. Biophys. Acta 464 (1977) 260–275.
[20] H. Binder, O. Zschörnig, The effect of metal cations on the phase behavior and hydration characteristics of phospholipid membranes, Chem. Phys. Lipids 115 (2002) 39–61.
[21] A. Cordomi, O. Edholm, J.J. Perez, Effect of ions on a dipalmitoyl phosphatidylcholine bilayer. A molecular dynamics simulation study, J. Phys. Chem. B 112 (2008) 1397–1408.
[22] S.A. Pandit, D. Bostick, M.L. Berkowitz, Molecular dynamics simulation of a dipalmitoylphosphatidylcholine bilayer with NaCl, Biophys. J. 84 (2003) 3743–3750.
[23] M. Eisenberg, T. Gresalfi, T. Riccio, S. McLaughlin, Adsorption of mono-valent cations to bilayer membranes containing negative phospholipids, Biochemistry 18 (1979) 5213–5223.
[24] H. Hauser, G.G. Shipley, Interactions of mono-valent cations with phosphatidylserine bilayer-membranes, Biochemistry 22 (1983) 2171–2178.
[25] J. Mattai, H. Hauser, R.A. Demel, G.G. Shipley, Interactions of metal-ions with phosphatidylserine bilayer-membranes — effect of hydrocarbon chain unsaturation, Biochemistry 28 (1989) 2322–2330.
[26] P. Mukhopadhyay, L. Monticelli, D.P. Tieleman, Molecular dynamics simulation of a palmitoyl-oleoyl phosphatidylserine bilayer with Na^+ counterions and NaCl, Biophys. J. 86 (2004) 1601–1609.
[27] U.R. Pedersen, C. Leidy, P. Westh, G.H. Peters, The effect of calcium on the properties of charged phospholipid bilayers, Biochim. Biophys. Acta, Biomembr. 1758 (2006) 573–582.
[28] S.A. Pandit, D. Bostick, M.L. Berkowitz, Mixed bilayer containing dipalmitoylphosphatidylcholine and dipalmitoylphosphatidylserine: lipid complexation, ion binding, and electrostatics, Biophys. J. 85 (2003) 3120–3131.
[29] T. Broemstrup, N. Reuter, Molecular dynamics simulations of mixed acidic/zwitterionic phospholipid bilayers, Biophys. J. 99 (2010) 825–833.
[30] J.M. Ruso, L. Besada, P. Martinez-Landeira, L. Seoane, G. Prieto, M. Sarmiento, Interactions between liposomes and cations in aqueous solution, J. Liposome Res. 13 (2003) 131–145.
[31] K. Murzyn, T. Róg, M. Pasenkiewicz-Gierula, Phosphatidylethanolamine–phosphatidylglycerol bilayer as a model of the inner bacterial membrane, Biophys. J. 88 (2005) 1091–1103.
[32] P. Jurkiewicz, J. Sýkora, A. Olžyńska, J. Humpolíčková, M. Hof, Solvent relaxation in phospholipid bilayers: principles and recent applications, J. Fluoresc. 15 (2005) 883–894.
[33] M.L. Horng, J.A. Gardecki, A. Papazyan, M. Maroncelli, Subpicosecond measurements of polar solvation dynamics — coumarin-153 revisited, J. Phys. Chem. 99 (1995) 17311–17337.
[34] R.S. Fee, M. Maroncelli, Estimating the time-zero spectrum in time-resolved emission measurements of solvation dynamics, Chem. Phys. 183 (1994) 235–247.
[35] O. Berger, O. Edholm, F. Jähnig, Molecular dynamics simulations of a fluid bilayer of dipalmitoylphosphatidylcholine at full hydration, constant pressure, and constant temperature, Biophys. J. 72 (1997) 2002–2013.
[36] H.J.C. Berendsen, J.P.M. Postma, W.F. van Gunsteren, J. Hermans, Interaction models for water in relation to protein hydration, in: B. Pullman (Ed.), Intermolecular Forces, D. Reidel Publishing Company, Dordrecht, 1981, pp. 331–342.
[37] B. Hess, C. Kutzner, D. van der Spoel, E. Lindahl, GROMACS 4: algorithms for highly efficient, load-balanced, and scalable molecular simulation, J. Chem. Theory Comput. 4 (2008) 435–447.
[38] R. Vacha, M.L. Berkowitz, P. Jungwirth, Molecular model of a cell plasma membrane with an asymmetric multicomponent composition: water permeation and ion effects, Biophys. J. 96 (2009) 4493–4501.
[39] W.G. Hoover, Canonical dynamics — equilibrium phase-space distributions, Phys. Rev. A 31 (1985) 1695–1697.
[40] M. Parrinello, A. Rahman, Polymorphic transitions in single-crystals — a new molecular-dynamics method, J. Appl. Phys. 52 (1981) 7182–7190.
[41] T. Darden, D. York, L. Pedersen, Particle mesh Ewald — an N.log(N) method for Ewald sums in large systems, J. Chem. Phys. 98 (1993) 10089–10092.
[42] S. Miyamoto, P.A. Kollman, Settle — an analytical version of the SHAKE and RATTLE algorithm for rigid water models, J. Comput. Chem. 13 (1992) 952–962.
[43] B. Hess, H. Bekker, H.J.C. Berendsen, J. Fraaije, LINCS: a linear constraint solver for molecular simulations, J. Comput. Chem. 18 (1997) 1463–1472.
[44] P. Jurkiewicz, A. Olžyńska, M. Langner, M. Hof, Headgroup hydration and mobility of DOTAP/DOPC bilayers: a fluorescence solvent relaxation study, Langmuir 22 (2006) 8741–8749.
[45] J. Barucha-Kraszewska, S. Kraszewski, P. Jurkiewicz, C. Ramseyer, M. Hof, Numerical studies of the membrane fluorescent dyes dynamics in ground and excited states, Biochim. Biophys. Acta, Biomembr. 1798 (2010) 1724–1734.
[46] J. Sýkora, P. Kapusta, V. Fidler, M. Hof, On what time scale does solvent relaxation in phospholipid bilayers happen? Langmuir 18 (2002) 571–574.
[47] A. Olžyńska, A. Zań, P. Jurkiewicz, J. Sýkora, G. Gröbner, M. Langner, M. Hof, Molecular interpretation of fluorescence solvent relaxation of Patman and H-2 NMR experiments in phosphatidylcholine bilayers, Chem. Phys. Lipids 147 (2007) 69–77.
[48] C.F. Schmidt, Y. Barenholz, C. Huang, T.E. Thompson, Phosphatidylcholine carbon-13-labeled carbonyls as a probe of bilayer structure, Biochemistry 16 (1977) 3948–3954.
[49] A.A. Gurtovenko, Asymmetry of lipid bilayers induced by monovalent salt: atomistic molecular-dynamics study, J. Chem. Phys. 122 (2005) 244902.
[50] S.J. Lee, Y. Song, N.A. Baker, Molecular dynamics simulations of asymmetric NaCl and KCl solutions separated by phosphatidylcholine bilayers: potential drops and structural changes induced by strong Na^+–lipid interactions and finite size effects, Biophys. J. 94 (2008) 3565–3576.
[51] E. Leontidis, A. Aroti, Liquid expanded monolayers of lipids as model systems to understand the anionic Hofmeister series: 2. Ion partitioning is mostly a matter of size, J. Phys. Chem. B 113 (2009) 1460–1467.
[52] B. Klasczyk, V. Knecht, R. Lipowsky, D. Dimova, Interactions of alkali metal chlorides with phosphatidylcholine vesicles, Langmuir 26 (2010) 18951–18958.